

# sim4dhs - Algorithm for the thermohydraulic simulation of district heating systems: Identification of optimal locations for additional heat sources

Pelda Johannes D.1; Holler Stefan1;

<sup>1</sup>University of Applied Sciences and Arts Hildesheim/Holzminden/Göttingen (HAWK), Göttingen in Germany;

\*corresponding author:

e-mail: johannes.pelda@hawk.de

#### **Abstract**

In 2023, renewables covered 22 % of Germany's final energy use - 53 % in electricity but only 18 % in heat, even though heat makes up half of total consumption. In particular, district heating promises a high potential of reducing CO<sub>2</sub> emissions.

In order to unlock this potential, district heating systems must adapt to the technical requirements of renewable energies in order to keep or even improve the efficiency of the system. Lowering the grid temperatures is the key, but old building structures limit the reduction of the return temperature. This leads to increased mass flow and pressure losses and thus to local bottlenecks. But could decentral integrated renewable heat sources alone be enough to avoid thermal-hydraulic bottlenecks?

This work presents sim4dhs, a non-convex MINLP model, that optimizes the locations of renewable heat sources so that as many extraction points as possible comply with the contractually required pressure differences.

Results show additional heat sources can reduce bottlenecks effectively, and pressure boosting eliminates them entirely. Optimal locations are often at subtree entrances or midpoints of districts.

**Keywords:** district heating, renewable energies, optimization, thermo-hydraulic simulation, pressure drop

#### 1. Introduction

In Germany, only 18 % of heat is generated from renewable energies, with the majority of heat coming from gas (40 %) and coal (22 %). [1]

Transforming DHS from fossil power towards renewable energy is challenging. Adapting temperature levels to renewables and old building structures lead to lower temperature spread at heat sinks, to increased mass flows and pressure losses.

This article aims to analyze the hydraulic effects and to evaluate the thermo-hydraulic impact of optimally integrating additional decentralized heat sources.

# 2. Materials and Methods

The mass flow at a heat source results from the inlet temperature, the outlet temperature and the heat load. Heat losses are taken into account. This results in a non-convex model that requires significantly more calculation time with increasing network elements. The network of the case study must therefore be simplified by splitting off sub-networks with an inlet pipe diameter of less than DN 80. Each sub-network is simulated separately across operating states by lowering the inlet temperature at the separation point in 1 K steps down to just above the return temperature. Regression functions are then derived to describe the thermo-hydraulic behavior, replacing each sub-network with an equivalent heat sink.

## 2.1. Case study

The case study is a slightly modified real DHN. Heat generator 2 has a fixed thermal feed-in capacity of 1 MW. The maximum feed-in capacity of the entire DHN is 16.7 MW. The case study consists of 2 heat sources, 315 heat sinks, 1,563 pipes and 1,565 nodes.

#### 2.1. Model

The base model consists of mass and energy balances at the nodes, equating incoming and outcoming mass and energy flows. Furthermore, each pipe inlet temperature is set to the upstream node's temperature by a complementary constraints formulation, the heat loss in each pipe is calculated by a linear approach and set equal to the difference between incoming energy and outgoing energy. Temperatures at the outlet of heat sources and heat sinks are fixed to 70 °C and 50 °C, respectively. Heat demand is set to year's peak demand.

The optimization model builds on the simulation model by adding an objective function to identify thermohydraulically optimal locations for new heat sources, aiming to reduce hydraulic bottlenecks caused by a smaller temperature spread. Only in the primary network additional heat sources can be installed between return nodes and their nearest supply node. For each possible location (1) and (2) determine whether there will be an additional heat source integrated.

$$\dot{\mathbf{m}}_{i} \ge \left(1 - \mathbf{z}_{i}\right) \cdot -\mathbf{M}_{i} \tag{1}$$

$$\dot{\mathbf{m}}_i \le \mathbf{z}_i \cdot \mathbf{M}_i \tag{2}$$

In which  $z_j$  are the binary variables,  $M_j$  are the Big-M values for  $j \forall j \in \mathcal{E}_{h,*}$  with upper bound of  $\dot{m}_j$ .

(3) sets the maximum number of additional heat sources.

$$\sum_{j \in \mathcal{E}_{h,*}} z_j \le |\mathcal{E}_{h,*}| \tag{3}$$

In which  $z_j$  are the binary variables defined in (1) and (2). In advance  $|\mathcal{E}_{h,*}|$  is determined between zero and five additional heat sources.

In the objective function (4),the sum of the product of pressure difference and heat extraction indicates how much heat is available at the heat sinks with sufficient pressure difference. (4) is minimized.

$$\sum_{j \in (\mathcal{E}_c \wedge \mathcal{E}_{c,*})} \Delta p_j \dot{Q}_j \tag{4}$$

In which  $\Delta p_j$  is the pressure drop and  $\dot{Q}_j$ , defined negative, is the thermal demand at the heat sinks  $j \in (\mathcal{E}_c \wedge \mathcal{E}_{c,*})$ , whereas  $\mathcal{E}_c$  are heat sinks in the primary network and  $\mathcal{E}_{c,*}$  are the artificial heat sinks each representing a sub-network by its regression function. Models are solved by solvers SCIP [4] and GUROBI [6].

#### 3. Results

Figure 1 illustrates how additional heat sources  $j \in \mathcal{E}_{h,*}$  influence the target function and supply security. Adding up to two heat sources significantly improves the pressure profile. Figure 2 illustrates the locations of additional heat sources and undersupplied heat sinks. Placements within sub-networks are not permitted.

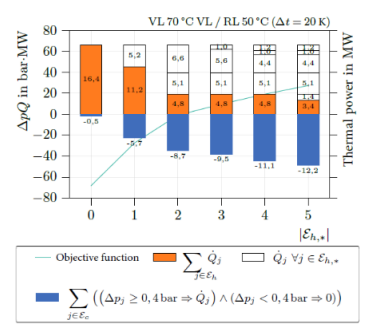


Figure 1: Progression of the target function  $(\Delta p \dot{Q})$ , the thermal power provided by the original heat sources  $(\dot{Q}_j)$  and the additionally installed thermal power  $(\mathcal{E}_{h,*})$ . The blue bar indicates heat delivered with a pressure drop of at least 0.4 bar at the customer stations. The maximum would be 16 MW. The locations of additional heat sources  $j \, \forall j \in \mathcal{E}_{h,*}$  do not change with increasing  $|\mathcal{E}_{h,*}|$ .

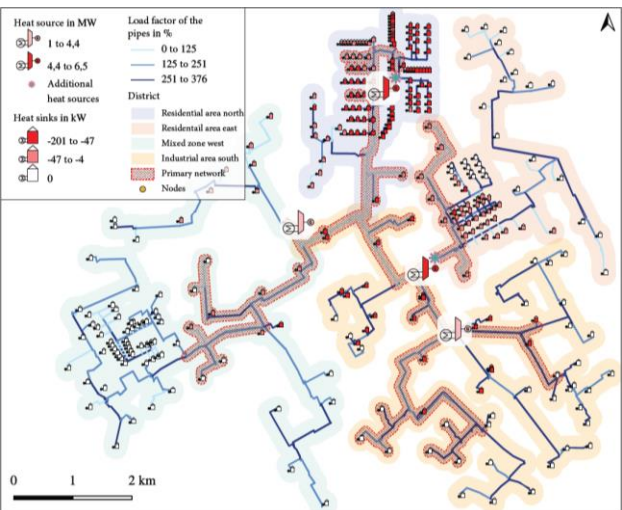


Figure 2: District heating network map of the 50/30/2 scenario.

From scenario 50/30/0 to 50/30/2, the pressure at the network's low point increases by 4.2 bar. As shown in

Figure 3, decentralized heat sources locally raise the pressure difference between supply and return lines.

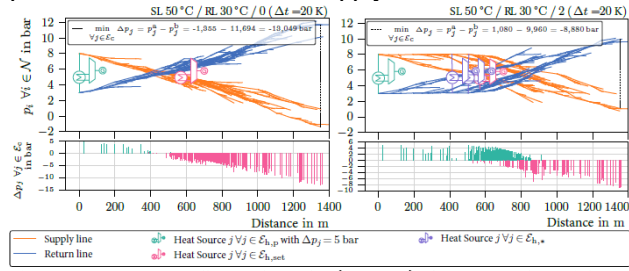


Figure 3: Pressure curve diagram by nodes  $(p_i \forall \in \mathcal{N})$ , the pressure-determining heat source  $\mathcal{E}_{h, p}$ , a heat-controlled heat source  $(\mathcal{E}_{h, set})$  and additional heat sources  $(\mathcal{E}_{h, *})$  integrated at optimum locations.

By extracting water from the return line, heating it, and injecting it into the supply line, they reduce mass flow and thus pressure loss between main and additional sources resulting in near-horizontal pressure gradient curves.

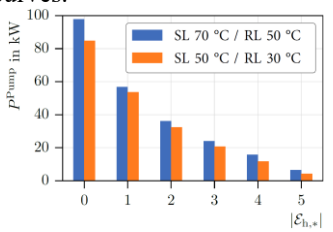


Figure 4 Minimum pump output  $(P^{Pump})$  required to fully supply all heat sinks in the network with a pressure difference of more than 0.4 bar.  $|E_{h,*}|$  is the number of additional heat sources installed.

Figure 4 shows that the first decentralized heat source halves the required pump capacity. Up to scenarios 70/50/2 and 50/30/2, pump power drops sharply from  $\sim 100 \, \mathrm{kW}$  to  $36 \, \mathrm{kW}$  and  $32 \, \mathrm{kW}$ , respectively, then levels off. The lower pump demand in 50/30/2 also reflects reduced heat losses.

# 4. Conclusion

The results show how a transformation of DHS into the 4th generation can be made thermo-hydraulically possible by integrating decentralized heat sources. Additional pumps are still required if peak heat demand is not reduced by refurbishment or peak load reduction due to load shift.

## References

- [1] AG Energiebilanzen, "Auswertungstabellen zur Energiebilanz Deutschland: Daten für die Jahre von 1990 bis 2023," Berlin, 2025.
- [2] M. Sameti and F. Haghighat, "Optimization approaches in district heating and cooling thermal network," *Energy and Buildings*, vol. 140, pp. 121–130, 2017, doi: 10.1016/j.enbuild.2017.01.062.
- [3] openmod-initiative, *Open Models*. [Online]. Available: https://wiki.openmod-initiative.org/wiki/Main\_Page (accessed: Nov. 10 2022).
- [4] G. Gamrath *et al.*, "The SCIP Optimization Suite 7.0," Technical Report, Optimization Online, 2020. [Online]. Available: http://www.optimization-online.org/DB\_ HTML/2020/03/7705.html
- [5] K. Bestuzheva et al., "The SCIP Optimization Suite 8.0," ZIB-Report, Zuse Institute Berlin 21-41, 2021. Accessed: Sep. 19 2023. [Online]. Available: http://nbn-resolving.de/urn:nbn:de:0297-zib-85309
- [6] Gurobi Optimization, LLC, Gurobi Optimizer Reference Manual. [Online]. Available: https:// www.gurobi.com/documentation/current/refman/ index.html (accessed: Mar. 27 2024).